A theoretical study of solvent effects on the $^1(n \to \pi^*)$ electron transition in acrolein

M. E. Martín, Aurora Muñoz Losa, I. Fdez.-Galván, and M. A. Aguilar[a]
Departamento Química Física, Universidad de Extremadura, 06071 Badajoz, Spain

The $^1(n \to \pi^*)$ electron transition of acrolein in liquid water was studied theoretically by using the averaged solvent electrostatic potential/molecular dynamics method. The model combines a multireference perturbational treatment in the description of the solute molecule with molecular dynamics calculations in the description of the solvent. We demonstrate the importance of the solvent electron polarization, bulk solvent effects, and the use of relaxed geometries in solution on the calculated solvent shift. It is also shown that the inclusion of the dynamic correlation does not change the solvent shift although it must be used to reproduce the transition energy. © *2004 American Institute of Physics.* [DOI: 10.1063/1.1775182]

I. INTRODUCTION

Acrolein or propenal is the smallest α–β-unsaturated carbonyl compound. The interaction between the carbonyl group and the CC double bond makes it a compound of marked interest from a spectroscopic and theoretical point of view. Its electronic spectrum has been extensively studied[1] by different spectroscopic techniques with Walsh[2] being one of the first authors to describe the complete absorption spectrum of acrolein. The UV spectra of this compound has also been studied theoretically with *ab initio*[3–6] and semiempirical methods,[7,8] and both the lowest excited states and the high-energy part of the electronic spectrum have been characterized. The effect of solvation on the spectrum has been also studied by using a supermolecule approach[7] and with the RISM–SCF method[4] and, more recently, with continuum models[5,6] and a hybrid continuum/discrete solvent model.[5]

Traditionally, two strategies have been followed in the study of the solvent effect on electron spectra. In the first, continuum methods,[9] the solvent is characterized by its dielectric constant and index of refraction. In the second, quantum mechanics/molecular mechanics (QM/MM) methods,[10] one uses a discrete classical field to represent the solvent. Continuum methods, even if they constitute a good qualitative approach to the chemistry of the process being studied, neglect the microscopic structure of the solvent around the solute and consequently cannot take specific interactions into account. QM/MM methods fill this gap and provide a very detailed description of the solvent structure. However, the large number of quantum calculation involved means that the calculation level has to be restricted.

In previous papers[11] we have presented a useful method for the study of solvent effects on electron spectra. This method alternates high-level quantum calculations and molecular dynamics (MD) calculations in an iterative procedure. The main characteristic of the proposed method is that the solvent perturbation is introduced into the solute molecular Hamiltonian in an averaged way, i.e., we use a mean field approximation. The basic quantity in the model is the averaged value of the solvent electrostatic potential (ASEP). Our approach, referred to as ASEP/MD,[12] enables one to simultaneously optimize the solute charge distribution in solution and the solvent structure around it. Another important advantage of the method is that the electron degrees of freedom of the solvent respond instantaneously to the change in the solute charge distribution during the transitions, i.e., the electron solvent polarization is always in equilibrium with the solute charge distribution. The method has been implemented at the multiconfigurational self-consistent-field (MCSCF) level and has proven its utility in the study of the vertical electronic spectra for formaldehyde, acetaldehyde, and acetone in aqueous solution.[11(b)]

As application of the method, in this paper we study the solvent effect on a part of the *trans*-acrolein absorption spectra, that corresponding to the vertical $^1(n - \pi^*)$ electron transition. The *s-trans* isomer was selected because both theoretical and experimental results coincide in indicating that this is the most stable isomer. The vertical $^1(n - \pi^*)$ transition was preferred because it involves an appreciable charge displacement that, as has been theoretically[4–6,8] and experimentally[1(e)] proven, originates a blueshift. We shall try to analyze the solvent structure around the solute molecule and how it determines the nature and magnitude of the solvent shift. The rest of the paper is organized as follows: in Sec. II we explain the procedure followed in the calculation of the solvent shift. Computational details are described in Sec. III; Sec. IV presents numerical results and their discussion.

II. METHOD

ASEP/MD is a QM/MM method that makes use of the mean field approximation. Its main characteristics have been described elsewhere.[12] Here, we shall detail only those points pertinent to the current study.

The determination of solvent shifts with the ASEP/MD method involves two self-consistent processes. In the first, the solvent structure and the charge distribution and geom-
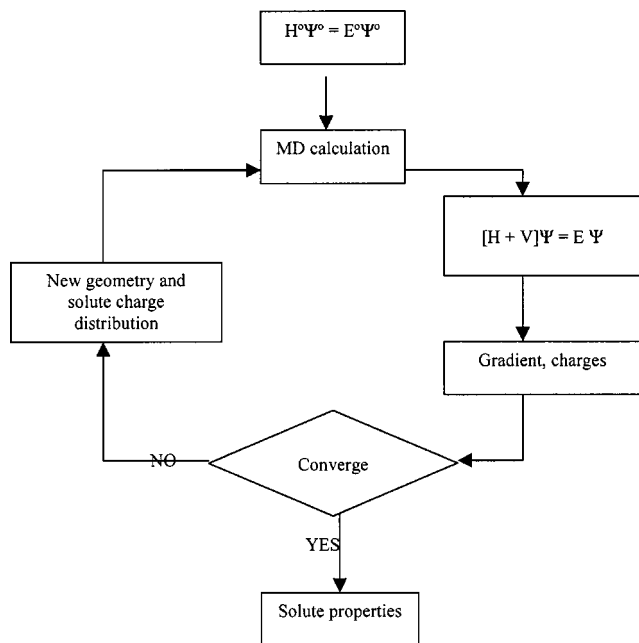
[a] Electronic mail: maguilar@unex.es

FIG. 1. ASEP/MD scheme.

etry of the solute become mutually equilibrated. In the second, the solvent electron polarization responds to the changes in the solute charge distribution originated by the electron transition.

As indicated above, ASEP/MD alternates high-level quantum calculations and molecular dynamics calculations in an iterative procedure. During the MD simulation the geometry and charge distribution of the solute and solvent molecules are considered as fixed. From the MD data one obtains the averaged solvent electrostatic potential that is introduced as a perturbation into the solute molecular Hamiltonian. By solving the associated Schrödinger equation, one gets a new solute charge distribution that serves as input for a new MD calculation. The process terminates when convergence in the solute charges and in the solute energy is reached. The procedure is described in Fig. 1. The charges that represent the chromophore molecule during the MD simulation were obtained from the solution solute molecule wave function by using the CHELPG method.[13]

The geometry of the acrolein molecule was optimized both in vacuo and in solution. In the latter case, we used a technique described in a previous paper[14] and based on the use of the free-energy gradient method.[15-17] At each step of the ASEP/MD cycle the total gradient, F, and the Hessian, H, were calculated as the sum of the solute and solvent contributions and used to obtain a new geometry through the expression $r_{k+1}=r_k+H_k^{-1}F_k$. This expression was used iteratively until the gradient converged. The new geometry was then used to represent the solute molecule during the MD calculation.

When one is interested in the study of electronic transitions it is necessary to perform an additional self-consistent process. Using the solvent structure and solute geometry obtained in the first self-consistent process, we couple the quantum mechanical solute and the electron polarization of the solvent. To this end, we assigned a molecular polarizabil-

ity to every water molecule, and simultaneously, replaced the effective water charge distribution used in the MD calculation (TIP3P for instance) by the gas phase values of the water molecule. The dipole moment induced on each solvent molecule is a function of the dipole moments induced on the rest of the molecules and of the solute charge distribution, and hence the electrostatic equation has to be solved self-consistently. The process finishes when convergence in the solute and solvent charge distribution is achieved. During the electron transition we apply the Franck–Condon principle, hence, we consider as fixed the solute geometry and the solvent structure around it. However, one permits the electron degrees of freedom of the solvent to respond to the change in the solute charge distribution.

The total energy of the system (quantum solute +polarizable solvent) is obtained as[10(j),10(k)]

$$U=U_{qq}+U_{pq}+U_{pp}+U_{\rho q}+U_{\rho p}+U_{\text{dist}}^{\text{solute}}+U_{\text{dist}}^{\text{solv}}.\qquad(1)$$

Here, q refers to the permanent charges of solvent molecules, p to the solvent induced dipoles, and ρ is the solute charge density. The two last terms in Eq. (1) are the distortion energies of the solute and solvent molecules, respectively, i.e., the energy spent in polarizing them. The different contributions are

$$U_{qq}=\frac{1}{2}\sum_i q_i V_i^q,\quad U_{pq}=-\sum_i \vec{p}_i\cdot\vec{E}_i^q,$$

$$U_{pp}=-\frac{1}{2}\sum_i \vec{p}_i\cdot\vec{E}_i^p,$$

$$U_{\text{dist}}^{\text{solv}}=\sum_i \frac{\vec{p}_i\vec{\alpha}_i^{-1}\vec{p}_i}{2}=\frac{1}{2}\sum_i \vec{p}_i\cdot\vec{E}_i$$

$$=\frac{1}{2}\sum_i \vec{p}_i[\vec{E}_i^q+\vec{E}_i^p+\vec{E}_i^p]$$

$$=-\frac{1}{2}U_{pq}-U_{pp}-\frac{1}{2}U_{\rho p},$$

$$U_{\rho q}=\sum_i q_i V_i^\rho,\quad U_{\rho p}=-\sum_i \vec{p}_i\vec{E}_i^\rho,\qquad(2)$$

$$U_{\text{dist}}^{\text{solute}}=\langle\Psi|H_{QM}|\Psi\rangle-\langle\Psi^0|H_{QM}|\Psi^0\rangle,$$

where Ψ and Ψ^0 are the in solution and in vacuo solute wave functions, respectively. V_i^ρ and V_i^q are the electrostatic potential generated by the solute charge distribution and by the permanent charges of the solvent, respectively. The electric field generated by the solute, solvent permanent charges, and solvent induced dipoles are, respectively, $\vec{E}_i^\rho$, $\vec{E}_i^q$, and $\vec{E}_i^p$. The terms that involve the solute molecule are calculated quantum mechanically. The final expression for the total energy of the system is

$$U=U_{qq}+\tfrac{1}{2}U_{pq}+U_{\rho q}+\tfrac{1}{2}U_{\rho p}+U_{\text{dist}}^{\text{solute}}.\qquad(3)$$

Once the solvation energy has been calculated for the ground and excited states, the solvent shift can be obtained as the difference,

$$\delta=U_{ex}-U_g=\tfrac{1}{2}\delta_{pq}+\delta_{\rho q}+\tfrac{1}{2}\delta_{\rho p}+\delta_{\text{dist}}^{\text{solute}}.\qquad(4)$$

The term δ_{qq} cancels out because, in vertical transitions where the Franck–Condon approximation is applicable, the U_{qq} term takes the same value in both the ground and the excited state. From a practical point of view the Franck–Condon approximation implies that the first self-consistent process (with or without geometry optimization) is carried out just for the ground state. However, the second cyclic process that permits the response of the electronic degrees of freedom of the solvent is carried out for both the ground and excited states. We would like to remark that in the previous version of the method[9] the δ_{pq} term was missing. As shown below, this term is not negligible and its contribution to the total solvent shift can be appreciable.

III. COMPUTATIONAL DETAILS

We applied the ASEP/MD methodology to study the $^1(n \to \pi^*)$ transition in the *trans*-acrolein molecule. Ground and excited states were described using the CASSCF level of theory with dynamic correlation energy calculated with second-order perturbation theory (CASPT2). The complete active space is spanned by all the configurations arising from six valence electrons in five orbitals ($6e/5o$). Contracted basis functions based on atomic natural orbitals[18] (ANO) were used in the calculations. The contraction scheme used was C,O[$4s3p1d$]/H[$2s1p$]. The initial geometry for acrolein was obtained by CASSCF optimization, in vacuo, with the aforementioned basis set. Two sets of calculations were performed. In the first, the geometries optimized in vacuo (hereafter Geom1) were used for the computations in solution. In the second, in solution geometry optimization was allowed (hereafter Geom2).

The MD simulations were performed using the program MOLDY.[19] The solvent was represented by 214 TIP3P[20] water molecules at fixed intramolecular geometry in a cubic box of 18.7 Å. The solute parameters were obtained by combining Lennard-Jones interatomic interactions[21] with electrostatic interactions. Periodic boundary conditions were applied and spherical cutoffs were used to truncate the acrolein–water interactions at 9 Å. The electrostatic interaction was calculated with the Ewald method. The temperature was fixed at 298 K by using the Nosé–Hoover[22] thermostat. Each simulation was run for 150 000 time steps where 50 000 were employed for equilibration and the 100 000 for production. A time step of 0.5 fs was used.

During the ASEP/MD cycle, the quantum calculations were performed at the CASSCF level of theory using the GAUSSIAN98 package[23] of programs. However, it is known[24] that to describe correctly electron transitions in conjugated molecules one must include the dynamic correlation contribution. Hence, once we had obtained the solvent structure around the solute, we used the CASPT2 method included in MOLCAS-5[25] to recalculate the transition energies and solvent shift values.

IV. RESULTS

In this section we present the results of the study of the $n \to \pi^*$ transition of the conjugated system, both in gas phase and in water liquid.

TABLE I. Gas phase dipole moments of acrolein (in Debyes).

	Other authors		
	$\mu^{0\,a}$	$\mu^{0\,b}$	μ^0(exp)
Ground state	3.03	3.06	2.90
Excited state	0.91	1.53	

[a]This work.
[b]Thakur *et al.* [Ref. 7(c)].

A. Gas phase

The transition energy in vacuo was calculated to be 3.97 eV at the CASSCF level and 3.69 eV at CASPT2 (using a two-roots state-average zero-order wave function). These results are in very good agreement with experiment that places this band between 3.71 (Ref. 2) and 3.75 [Ref. 1(c)] eV. Clearly, the inclusion of the dynamic correlation component is compulsory if one desires to reproduce the transition energy. Our results are almost coincident with those of Aquilante *et al.*,[5] who employed the same level of calculations but a basis set where supplementary diffuse functions were included in order to describe Rydberg states, and close to those obtained by Andrade do Monte *et al.*,[6] 3.74 and 3.85 eV at MR–CISD and MR–CISD–Q levels, respectively.

Table I lists the dipole moments obtained in the present study as well as those calculated by other workers and the experimental values, when available. The ground state dipole moment, 3.03 D, is only slightly higher than the experimental value, 2.90 D,[26] and of the same order of magnitude as that published by Thakur *et al.*[7(c)] in a semiempirical study. When the $n \to \pi^*$ transition takes place, a major change in the solute charge distribution occurs, the dipole moment of the excited state decreases sharply, and hence a strong blueshift is expected if the system is immersed in a polar solvent. This decrease of the dipole moment is not well reproduced by the semiempirical method.

B. Aqueous solution

We begin by analyzing the changes induced by the solvent on the solute geometry (see Fig. 2). As expected, the main changes are located in the molecular section close to the more polar group, the carboxylic bond. In particular, the C–O bond length increases while the C1–C2 and C1–H lengths decrease. This behavior may be because solution increases the contribution of the zwitterionic form of the CO bond.
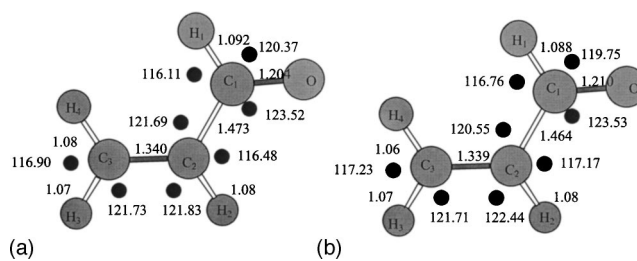

FIG. 2. (a) gas phase geometry; (b) in solution geometry.

J. Chem. Phys., Vol. 121, No. 8, 22 August 2004

Solvent effects on the $^1(n\rightarrow\pi^*)$ transition in acrolein   3713

TABLE II. In solution dipole moment of acrolein (in Debyes).

	μ_g	μ_e	$\Delta\mu_g = \mu_g - \mu_g^0$	$\Delta\mu_e = \mu_e - \mu_e^0$
Geom 1	4.00±0.12	1.76±0.11	0.97	0.85
Geom 2	3.98±0.05	1.79±0.09	0.95	0.88

Next, we analyze the polarization of the acrolein molecule in liquid water. Table II displays the in solution total and induced dipole moments in both the ground and excited state. The ground state dipole moment evolution during the self-consistent ASEP/MD process is shown in Fig. 3. One observes that the dipole moment increases until convergence is achieved. Then it begins to fluctuate around an average value of 4.00±0.11 D (Geom1) or 3.98±0.07 D (Geom2). These values (and the rest of the mean values given in the paper) were calculated as the mean value over the last 10 ASEP/MD cycles, i.e., 500 ps. We also give the rms values. Even if the dipole fluctuations could be decreased by increasing the length of the simulation time, our experience indicates that the average value will stay nearly constant. The use of the optimized geometry in solution or in vacuo hardly influences the dipole moment values. The solvent perturbation, however, increases dramatically the dipole moment values, by 32% in the ground state case and by 90% in the excited state. The difference between the dipole moments of the ground and excited states (which is important because it determines the solvent shift) increases only slightly in solution, passing from 2.12 D (in vacuo) to 2.24 D (in solution, Geom1) or 2.19 D (in solution, Geom2). Figure 4 shows the atomic charges for the acrolein molecule in vacuo and in solution for the ground and excited states. In solution, the charges on the atoms of the carboxylic group in the ground state increase by about 20%. When excited, the charge on the C atom of the carboxylic group disappears, and the charge on the oxygen atom is clearly reduced, although this effect is somewhat lower in solution. From these data one can expect that the blue solvent shift of the $n\rightarrow\pi^*$ transition will be electrostatic in origin.

To understand further the nature of the solvent shift it is interesting to analyze the solvent structure around the acrolein molecule. The radial distribution functions oxygen (water)–oxygen (acrolein) and hydrogen (water)–oxygen (acrolein) are shown in Figs. 5 and 6, respectively. They were obtained as average values over the last 10 ASEP/MD cycles. The H(w)–O(a) radial distribution function (rdf) displays a well defined peak at 1.85 Å, indicating a strong
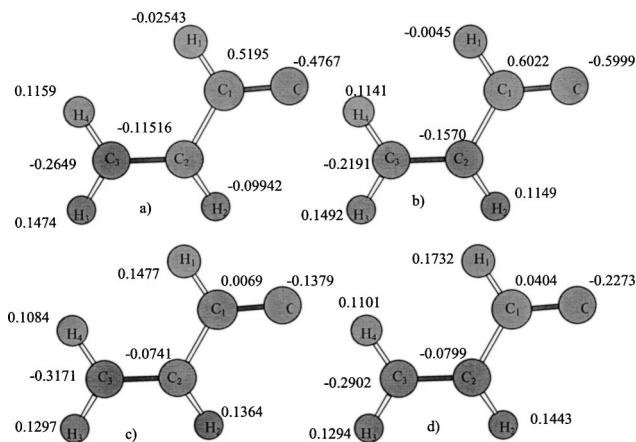
FIG. 4. (a) S_0 acrolein charge distribution in gas phase; (b) S_0 acrolein charge distribution in water solution; (c) S_1 acrolein charge distribution in gas phase; (d) S_1 acrolein charge distribution in aqueous solution.

hydrogen bond between acrolein and a water molecule. The first peak of the O(w)–O(a) rdf appears at 2.75 Å, and given that the H–O distance in water is 0.957 Å, one can conclude that the hydrogen bond is almost linear. In Fig. 5, it can also be observed that the radial distribution function has several peaks at long distances, indicating that acrolein imposes a considerable order on the water structure. The calculated coordination number is 2.1. The two pairs of free electrons of the acrolein oxygen are involved in the formation of hydrogen bonds. These conclusions are independent of the geometry used for the acrolein molecule.

Table III lists the solvent shift and its different contributions [see Eq. (4)]. The first column corresponds to the solvent shift due to the electrostatic interaction between the solute charge distribution and the permanent charges of the solvent. The second and third columns correspond to the interaction between the induced solvent dipoles and the solute charge distribution and permanent solvent charges. The fourth column is the contribution of the solute distortion energy. The total solvent shift is given in the last column. The largest contribution to the solvent shift comes from the interaction between the solute and the permanent charges of the solvent. However, the contribution of the solvent polarization (components associated to the induced dipoles) is also important, representing about 20–26% of the total solvent shift depending on the geometry used in the calculation.

The solvent shift is very sensitive to the geometry used in the calculation. When the geometry optimized in solution is used the solvent shift decreases by 1.8 kcal/mol, with re-
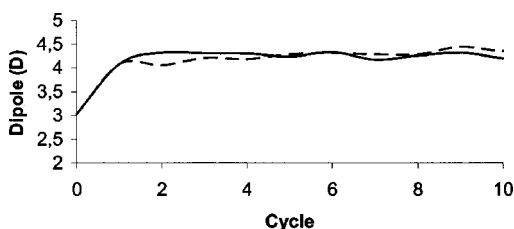

FIG. 3. Variation of the solute dipole moment as a function of the number of cycles of the ASEP/MD procedure. (Geom 1: dashed line, Geom 2: full line).
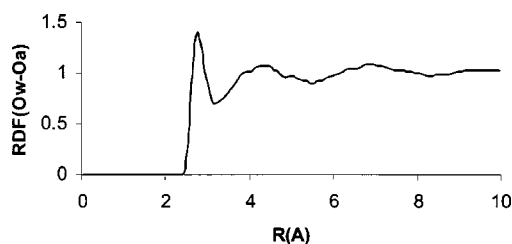

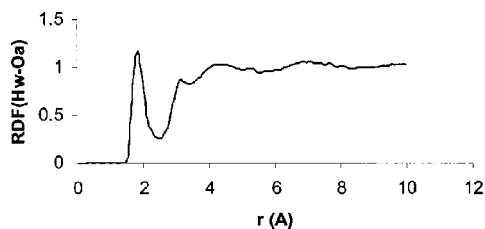FIG. 5. Oxygen (acrolein)–oxygen (water) radial distribution function.

FIG. 6. Oxygen (acrolein)–hydrogen (water) radial distribution function.

spect to the value obtained with the gas phase geometry. The analysis of the different components of the solvent shift shows that the solute–solvent and solvent–solvent interactions are not affected by the change of geometry, but the solute distortion energy changes appreciably. This component is the sum of two contributions, one associated to the distortion of the solute charge distribution during the polarization and the other to the distortion of the geometry during the solvation. As observed from Table II, the induced dipole moments (and hence the distortion of the solute charge distribution) are hardly affected by the change of geometry. We can hence conclude that the increase in the solute distortion component is directly associated to the distortion of the geometry. The explanation is that when the acrolein molecule passes from gas phase to solution the geometry of the ground state changes towards resembling the relaxed (n, π^*) in vacuo excited state geometry, i.e., increasing the double bond length and decreasing the C1–C2 distance. As a result, the total solvent shift is some 30% smaller than that obtained in the calculation with the gas phase geometry.

An interesting point to clarify is whether the solvent shift is a bulk solvent effect or it is associated to specific hydrogen bonds. To solve this question we recalculated the contribution to the solvent shift caused only by molecules belonging to the first solvation shell. We estimated the first shell contribution at 1.73 kcal/mol. This represents about 35% of the total solvent shift. However, the first shell accounted for about 80% of the induced dipole moment and 50% of the electrostatic solute–solvent interaction ($q\rho$ and $p\rho$ terms). These values imply that both components, bulk solvent and specific interactions, have to be considered in the determination of solvent shifts. A similar conclusion has been obtained by Canuto and co-workers in their studies of formaldehyde,[27] acetone,[28] and N-methyl acetamide[29] in aqueous solution. The first shell contribution to the solvent shift obtained with ASEP/MD is clearly lower than that obtained with a supermolecule approach[8] (between 4.3 and 6.9 kcal/mol depending on the basis set used). The reason is that the supermolecule method uses a fixed optimized geometry

for the water–acrolein system. In solution, however, the thermal agitation shifts the system from its optimal configuration, decreasing the solute–solvent interaction energy.

Next, we improved the calculation level by including the dynamic correlation energy of the solute. We used the CASPT2 method as implemented in the MOLCAS program package. When this component is included, the solvent shift values become 5.6 ± 0.5 kcal/mol (Geom1) and 4.5 ± 0.5 kcal/mol (Geom2). The experimental solvent shift for acrolein in water was estimated at 4.50 kcal/mol. The inclusion of dynamic correlation had a small effect on the solvent shift when Geom1 is used and is completely negligible in the case of Geom2. There was a noticeable effect of the dynamic correlation on the value of the transition energies both in vacuo and in solution. Inclusion of dynamic correlation at the CASPT2 level decreased the transition energies by about 4–5 kcal/mol. This effect, however, was similar in vacuo and in solution. As a consequence, the solvent shift (which is defined as the difference between the transition energy in solution and in vacuo) hardly depends on the inclusion of the dynamic correlation. The in solution transition energy is also very well reproduced. The experimental $n \to \pi^*$ band appears at 3.94 eV[1(e)] while the calculated value (Geom2) was 3.90 eV. A recent PCM–CASPT2 study by Aquilante et al.[5] provides a close value, 3.96 eV, for this magnitude. However, the calculated solvent shift, 7.6 kcal/mol when PCM was used and 9.9 kcal/mol when a hybrid continuum/discrete solvent model was used is too high. The overestimate of the solvent shift calculated by those authors may in part be due to the use of geometries optimized in vacuo for the computations in solution. Our results can serve to clarify this point. Our best value, 4.95 kcal/mol (Geom2), agrees with the experiment. However, if the geometry optimized in vacuo is used in the in solution calculation the difference increases to 1.6 kcal/mol. The use of in solution optimized geometries is a very important factor in the solvent shift determination, much more important than, for instance, the consideration of dynamic electron correlation. The same trend has been observed by Andrade do Monte et al.,[6] these authors studied the solvent influence on the acrolein spectra by using the COSMO continuum model and they also found that the use of in solution optimized geometries decrease the solvent shift in about 2 kcal/mol. The agreement between the results obtained with the two methods is interesting because the geometries used in the two cases were slightly different. In our calculation, the in solution geometry was obtained at CASSCF level that, as is well known,[30] underestimates the C–O distance. However, Andrade do Monte et al. optimized the geometry at DFT/B3LYP level obtaining somewhat bet-

TABLE III. Solvent shift and its components (in kcal/mol) calculated at CASSCF level.

	$\delta_{q\rho}$	$1/2\delta_{pq}$	$1/2\delta_{p\rho}$	δ_{dist}^{solute}	δ^a
Geom 1	6.0 ± 0.4	0.07 ± 0.05	1.09 ± 0.08	-1.1 ± 0.1	$6.1 \pm 0.5 (5.6 \pm 0.5)$
Geom 2	5.9 ± 0.4	0.04 ± 0.02	1.09 ± 0.05	-2.7 ± 0.4	$4.3 \pm 0.2 (4.5 \pm 0.2)$
First shell[b]	3.6 ± 0.2	-0.08 ± 0.07	0.40 ± 0.01	-2.1 ± 0.2	1.7 ± 0.2

[a]Values in parentheses calculated at CASPT2 level.
[b]Obtained with Geom 2.

ter geometries. So, the decreasing of the solvent shift when the geometry optimized in solution is used seems to be a consequence of the C–O bond lengthening, and not of the use of a specific geometry.

The agreement between the calculated and the experimental solvent shift is evidence for the electrostatic origin of the latter. The small difference may be due to the approximations introduced into the method (mean field approximation, potential parameters, etc.) and also to the contribution of the intermolecular electron correlation, i.e., the dispersion component. In the results presented in Table III this contribution is missing. The dispersion energy is responsible for the redshift that many molecules show in nonpolar solvents. In general, the solute polarizability takes larger values in the excited states than in the ground state. As a consequence, the dispersion component produces a redshift that in the case of carbonyl compounds opposes the electrostatic solvent shift. An exact (quantum mechanical) determination of this component is complicated due to the prohibitive number of excitations that must be included in the calculation of a system consisting of a solute and all the solvent molecules. Approximate formulas involve the determination of polarizabilities in the ground and excited states. However, the determination of exact polarizabilities of molecules in their excited states is far from trivial. For instance, if the polarizabilities are calculated at the CASSCF level and using the ANO basis sets indicated above, one gets 36.27 a.u. for the ground state and 36.26 a.u. for the excited state. These values seem to imply that for the acrolein–water system the contribution of the dispersion component to the solvent shift is small and furthermore it gives rise to a blueshift, something that opposes the abundant experimental information. Clearly, more detailed studies of the calculation of polarizabilities of excited states and of the evaluation of the dispersion component are needed.

V. CONCLUSIONS

The $^1(n \rightarrow \pi^*)$ transition in acrolein was studied in both gas and in solution phases. In both cases the calculated transition energies agreed very well with experiment. It is well established that CASPT2 calculations with ANO basis sets permit one to reproduce adequately the electron spectra of molecules. Additionally, in this work we have shown that the combination of this method and the ASEP/MD procedure permits one to describe adequately in solution transitions. With respect to the solvent shift, it was shown that while the inclusion of the dynamic correlation does not change the calculated value, the use of geometries optimized in solution is important. Small changes in the geometry, mainly of the carbonyl group, can dramatically modify the magnitude of the solvent shift. The analysis of the different solvent shift components showed how important it is to take the solvent electron polarization into consideration. Finally, in this present case of acrolein, both bulk solvent and specific interactions make major contributions to the calculated solvent shift.

[1] (a) J. C. D. Brand and D. G. Williamson, Discuss. Faraday Soc. **35**, 184 (1963); (b) J. M. Hollas, Spectrochim. Acta **19**, 1425 (1963); (c) R. S. Becker, K. Inuzuka, and J. King, J. Chem. Phys. **52**, 5164 (1970); (d) G. A. Osborne and D. A. Ramsay, Can. J. Chem. **51**, 1170 (1973); (e) A. E. Moskvin, Theor. Exp. Chem. **2**, 175 (1966).

[2] A. D. Walsh, Trans. Faraday Soc. **41**, 498 (1945).

[3] E. R. Davidson and L. E. Nitzsche, J. Am. Chem. Soc. **101**, 6524 (1979); K. Valenta and F. Grein, Can. J. Chem. **60**, 601 (1982); C. E. Dykstra, J. Am. Chem. Soc. **98**, 7182 (1976); A. Devaquet, *ibid.* **94**, 5160 (1972); M. Reguero, M. Olivucci, F. Bernardi, and M. A. Robb, *ibid.* **115**, 3710 (1993).

[4] S. Ten-no, F. Hirata, and S. Kato, J. Chem. Phys. **100**, 7443 (1994).

[5] F. Aquilante, V. Barone, and B. O. Roos, J. Chem. Phys. **119**, 12323 (2003).

[6] S. Andrade do Monte, T. Müller, M. Dallos, H. Lischka, M. Diedenhofen, and A. Klamt, Theor. Chem. Acc. **111**, 78 (2004).

[7] (a) C. Fridh, L. Åsbrink, and E. Lindholm, Phys. Scr. **20**, 603 (1979); (b) W. Haque, J. Chem. Phys. **67**, 3629 (1977); (c) S. Thakur, V. P. Gupta, and B. Ram, Spectrochim. Acta, Part A **53**, 749 (1997).

[8] S. Iwata and K. Morokuma, J. Am. Chem. Soc. **97**, 966 (1975).

[9] J. Tomasi, R. Bonaccorsi, R. Cammi, and F. J. Olivares del Valle, J. Mol. Struct.: THEOCHEM **234**, 401 (1991); J. Tomasi and M. Persico, Chem. Rev. (Washington, D.C.) **94**, 2027 (1994); J. L. Rivail and D. Rinaldi, in *Computational Chemistry: Review of Current Trends*, edited by J. Leszczynski (World Scientific, Singapore, 1995); C. J. Cramer and D. G. Truhlar, in *Reviews in Computational Chemistry*, edited by K. B. Lipkowitz and D. B. Boyd (VCH, New York, 1995), Vol. VI, p. 1; A. Klamt and J. Schüürmann, J. Chem. Soc., Perkin Trans. 2 **1993**, 799 (1993); T. N. Truong and E. V. Stefanovich, Chem. Phys. Lett. **240**, 253 (1995).

[10] (a) A. Warshel and M. Levitt, J. Mol. Biol. **103**, 227 (1976); (b) M. J. Field, P. A. Bash, and M. Karplus, J. Comput. Chem. **11**, 700 (1990); (c) V. Luzhkov and A. Warshel, *ibid.* **13**, 199 (1992); (d) J. Gao, J. Phys. Chem. **96**, 537 (1992); (e) M. A. Thompson, E. D. Glendening, and D. Feller, *ibid.* **98**, 10465 (1994); (f) D. Wei and D. R. Salahub, Chem. Phys. Lett. **224**, 291 (1994); (g) I. Tuñón, M. T. C. Martins-Costa, C. Millot, M. F. Ruiz-López, and J.-L. Rivail, J. Comput. Chem. **17**, 19 (1996); (h) T. A. Wesolowski and A. Warshel, J. Phys. Chem. **97**, 8050 (1993); **98**, 5183 (1994); (i) R. V. Stanton, L. R. Little, and K. M. Merz, *ibid.* **99**, 17344 (1995); (j) J. L. Gao, J. Comput. Chem. **18**, 1061 (1997); (k) M. A. Thompson, J. Phys. Chem. **100**, 14492 (1996).

[11] (a) M. L. Sánchez, M. E. Martín, M. A. Aguilar, and F. J. Olivares del Valle, Chem. Phys. Lett. **310**, 195 (1999); (b) M. E. Martín, M. L. Sánchez, F. J. Olivares del Valle, and M. A. Aguilar, J. Chem. Phys. **113**, 6308 (2000).

[12] M. L. Sánchez, M. A. Aguilar, and F. J. Olivares del Valle, J. Comput. Chem. **18**, 313 (1997); M. L. Sánchez, M. E. Martín, M. A. Aguilar, and F. J. Olivares del Valle, *ibid.* **21**, 705 (2000); A. Muñoz Losa, I. Fdez. Galván, M. E. Martín, and M. A. Aguilar, J. Phys. Chem. B **107**, 5043 (2003); M. L. Sánchez, M. E. Martín, I. Fdez. Galván, F. J. Olivares del Valle, and M. A. Aguilar, *ibid.* **106**, 4813 (2002); I. Fdez. Galván, M. L. Sánchez, M. E. Martín, F. J. Olivares del Valle, and M. A. Aguilar, Comput. Phys. Commun. **155**, 244 (2003).

[13] L. E. Chirlian and M. M. Francl, J. Comput. Chem. **8**, 894 (1987); C. M. Breneman and K. B. Wiberg, *ibid.* **11**, 316 (1990).

[14] I. Fdez. Galván, M. L. Sánchez, M. E. Martín, F. J. Olivares del Valle, and M. A. Aguilar, J. Chem. Phys. **118**, 255 (2003).

[15] N. Okuyama-Yoshida, M. Nagaoka, and T. Yamabe, Int. J. Quantum Chem. **70**, 95 (1998).

[16] N. Okuyama-Yoshida, K. Kataoka, M. Nagaoka, and T. Yamabe, J. Chem. Phys. **113**, 3519 (2000).

[17] H. Hirao, Y. Nagae, and M. Nagaoka, Chem. Phys. Lett. **348**, 350 (2001).

[18] P.-O. Widmark, P.-Å. Malmqvist, and B. O. Roos, Theor. Chim. Acta **77**, 291 (1990).

[19] K. Refson, Comput. Phys. Commun. **126**, 310 (2000).

[20] W. L. Jorgensen, J. Chandrasekhar, J. D. Madura, R. W. Impey, and M. L. Klein, J. Chem. Phys. **79**, 926 (1983).

[21] W. L. Jorgensen, D. S. Maxwell, and J. Tirado-Rives, J. Am. Chem. Soc. **117**, 11225 (1996).

[22] W. G. Hoover, Phys. Rev. A **31**, 1 (1985).

[23] M. J. Frisch, G. W. Trucks, H. B. Schlegel *et al.*, GAUSSIAN 98, Gaussian, Inc., Pittsburgh, PA, 1998.

[24] B. O. Roos, M. P. Fülscher, P.-Å. Malmqvist, M. Merchán, and L. Serrano-Andrés, in *Quantum Mechanical Electronic Structure Calculations with Chemical Accuracy*, edited by S. R. Langhorff (Kluwer, Dordrecht, 1994).

[25] K. Andersson *et al.*, *MOLCAS Version 5.2* (University of Lund, Lund, Sweden, 2003).

[26] G. A. Oscipov and V. I. Minkin, *Handbook of Dipole Moments* (Vishchaya Shicola Press, Moscow, 1965, p. 72.

[27] K. Coutinho and S. Canuto, J. Chem. Phys. **113**, 9132 (2000).

[28] K. Coutinho and S. Canuto, J. Mol. Struct.: THEOCHEM **632**, 235 (2003).

[29] W. R. Rocha, K. J. De Almeida, K. Coutinho, and S. Canuto, Chem. Phys. Lett. **345**, 171 (2001).

[30] V. Molina and M. Merchan, J. Phys. Chem. **105**, 3745 (2001).